



# Effects of AlN hydrolysis on fractal geometry characteristics of residue from secondary aluminium dross using response surface methodology

Yong ZHANG, Zhao-hui GUO, Zi-yu HAN, Xi-yuan XIAO

School of Metallurgy and Environment, Central South University, Changsha 410083, China

Received 6 November 2017; accepted 29 March 2018

**Abstract:** The effects of aluminium nitride (AlN) hydrolysis on fractal geometry characteristics of residue from secondary aluminium dross were studied using response surface methodology. The results show that the fractal dimensions of the residue can be significantly influenced by the AlN hydrolysis from secondary aluminium dross. The hydrolysis of AlN in the dross was spontaneous under temperatures of 303–373 K. The actual fractal dimensions of residue were significantly affected by the liquid–solid ratio ( $p < 0.05$ ) and changed from 1.16 to 1.80, which accurately aligned with those from the calculations. Moreover, the fractal dimensions of residue were significantly affected by the interactions between hydrolysis temperature and hydrolysis time, liquid–solid ratio and hydrolysis time, respectively ( $p < 0.01$ ). The minimum fractal dimensions of the residue reached 1.15 under the optimized conditions, which included a hydrolysis temperature of 30 °C, liquid–solid ratio of 5 mL/g and hydrolysis time of 10 min. The results suggest that response surface methodology can guide in optimizing the conditions of AlN hydrolysis in order to obtain the minimum fractal dimensions of residue for improving the reutilization of the dross.

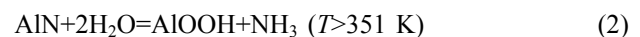
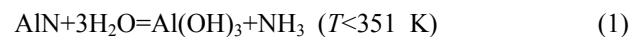
**Key words:** secondary aluminium dross; AlN hydrolysis; fractal dimensions; optimization; response surface methodology

## 1 Introduction

With the extensive development of the secondary aluminium industry, aluminium dross has been widely generated in China. However, more than 90% of the secondary aluminium dross has been disposed in landfills without further processing. The adverse effects of the dross on the natural environment have raised concern in recent years [1,2]. Secondary aluminium dross is a heterogeneous mixture that includes large lumps, fine oxides and small pieces of metals [3]. Most of the dross is a mixture of free metals and nonmetallic substances, including aluminium nitrides (e.g., aluminium oxide and salts) [4]. In Europe, it is forbidden to dispose waste in landfills due to the slag soluble salts that may surface in groundwater supplies [3]. Generally, the treatment of aluminium dross includes milling, shredding and subsequent granulometric classification [5]. The buried aluminium metal can react with alkaline material, forming the water soluble product  $[\text{Al}(\text{OH})_4]_{(\text{AQ})}^{-1}$  [6]. An effective method to extract the aluminium from the

aluminium dross is to use water as a solvent, as it is non-toxic and cheap. Thus, this technique is an environmentally friendly pretreatment method for the recycling of secondary aluminium dross.

The AlN in the dross can release ammonia gas when the dross is immersed in water, therefore, it is necessary to dispose the secondary aluminium dross [7], but the pretreated dross can be recycled as raw material for refractory bricks without releasing potential toxic and/or flammable gases [8–10]. Normally, AlN hydrolysis is significantly affected by the hydrolysis temperature, acidity of the solution and hydrolysis time. The hydrolysis of AlN can be considered as follows:



A crystalline bayerite is produced on the surface of the AlN particle when the hydrolysis temperature is below 351 K, while a crystalline boehmite is produced under hydrolysis temperatures greater than 351 K. Generally, AlN in solutions of HCl or NaOH is hydrolysed more efficiently than in solutions of

deionized water, while it is restrained in solutions of  $H_3PO_4$  [11,12]. However, the effects of AlN hydrolysis on fractal geometry characteristics of residue from secondary aluminium dross have rarely been studied.

The fractal characteristics of particle size distribution in dynamic flocculation processes can be optimized according to the addition of coagulants and the quality of outflow [13]. The mechanism governing the transport of particles is related to the fractal dimension, as the effective range decreases when the fractal dimension increases [14]. Based on fractal geometry and the constitutive equation of Herschel–Bulkley fluids, an analytical model of a Herschel–Bulkley fluid flowing in a porous geo-material with fractal characteristics was derived. The proposed model provides a theoretical basis for grouting design and helps in understanding chemical fluid flow in soil [15]. The multi-fractal boxing-counting method was used for the analysis of  $Al_2O_3$ ,  $Fe_2O_3$  and  $SiO_2$  contents of primary and accumulated bauxite ore from the Pingguo bauxite deposit, western Guangxi. The results show that the  $Al_2O_3$ ,  $Fe_2O_3$  and  $SiO_2$  contents of bauxite present a characteristic multi-fractal distribution. During the evolutionary process from a primary bauxite deposit to an accumulated bauxite ore,  $Al_2O_3$  and  $Fe_2O_3$  contents become enriched, while  $SiO_2$  content is depleted [16]. The large amount of residue still existed after AlN hydrolysis from secondary aluminium dross. As a practical response surface methodology model, the Doehlert model minimizes experimental points and maintains a high precision of prediction [17]. The leaching process used to extract Mn from a low-grade manganese ore was investigated using response surface experiments. The optimum conditions under which the Mn and Fe recoveries were the highest, as well as the time and temperature when these recoveries were the lowest, were determined using response surface design. The results show that Mn and Fe recoveries were 93.44% and 15.72% under the optimum conditions, respectively. The sulfuric acid concentration was the most effective parameter affecting the recovery process [18]. Microwaves were applied to roasting the zinc oxide fume obtained from fuming a furnace for the removal of F and Cl. The effects of important parameters, such as roasting temperature, holding time and stirring speed, were investigated and the process conditions were optimized using response surface methodology. The results show that the effects of roasting temperature and holding time on the removal rate of F and Cl are significant, and that of stirring speed follows in significance. During the roasting temperature of 700 °C, holding time of 80 min and stirring speed of 120 r/min, the defluorination rate reached 92.6% while the dechlorination rate reached 90.2% [19]. Response surface methodology was used to optimize the reduction roasting process for low-grade

pyrolusite using bagasse as the reducing agent, which had the mass ratio of 0.9:10, the roasting temperature of 450 °C and the roasting time of 30 min [20]. Response surface methodology was also used to build a predictive model of the combined effects of independent variables (including the microwave powder, the active time and the rotational frequency) for microwave drying of selenium-rich slag. During the optimum operating conditions of the microwave powder of 14.97 kW, the acting time of 89.58 min, the rotational frequency of 10.94 Hz, and the temperature of 136.407 °C, the relative dehydration rate of 97.1895% was obtained [21]. The results suggest that response surface methodology is a favourable technique widely applied in various engineering courses. This statistical design can accurately illustrate the interactions of variables and helps to identify the optimum conditions of variables, features which are ignored in traditional one-factor designs [17]. Another important advantage of response surface methodology is its potential to detect the effects of interactions between independent variables from the range studied to characterize the process. This methodology generates mathematical equations that allow a more detailed description of the studied process. However, it is insufficient to elucidate the relationship between homogenization of residue and the conditions of AlN hydrolysis from secondary aluminium dross using response surface methodology. Response surface methodology is more efficient and comprehensive than applying this statistical method in the effect of AlN hydrolysis on fractal geometry characteristics of residue from secondary aluminium dross.

In this work, the effects of AlN hydrolysis from secondary aluminium dross on fractal dimensions of residue using response surface methodology were studied. The objectives of this work were to: (1) study the fractal dimensions of residue from secondary aluminium dross after AlN hydrolysis using response surface methodology, (2) determine both the single factor and the interactive influences on the fractal dimensions of the residue and (3) elucidate the feasibility of the hydrolysis conditions of AlN, which was guided using response surface methodology in order to obtain the minimum fractal dimensions of residue for improving the reutilization of the dross.

## 2 Experimental

### 2.1 Materials

The secondary aluminium dross was collected from a secondary aluminium plant in Jiangxi Province of China. Prior to the experiment, the initial steps included cooling the hot dross, then crushing, grinding and downsizing it. After undergoing these mechanical

operations, approximately 92.40% of the dross particles had a size fraction of less than 41.84  $\mu\text{m}$  and the  $D_{50}$  value of 23.42  $\mu\text{m}$ . The dross was assigned with quartation for the AlN hydrolysis experiments. The dross samples were mainly composed of Al, Mg, Si and Ca (Table 1) and the main mineral phases of the dross included Al,  $\alpha\text{-Al}_2\text{O}_3$ ,  $\text{MgAl}_2\text{O}_4$  and AlN (Fig. 1).

**Table 1** Chemical composition of secondary aluminium dross (mass fraction, %)

Al	Mg	Si	Ca	Fe	Na	Ti	Others
39.61	6.39	7.26	3.47	1.20	1.03	1.61	39.43

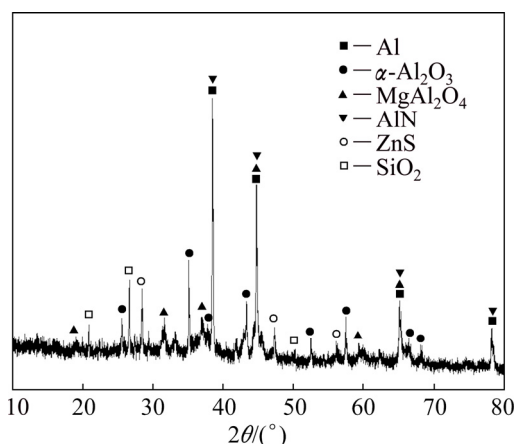


**Fig. 1** XRD pattern of dross

## 2.2 Experimental design

Experiments were set up using the Design Expert software [18]. The independent variables, such as hydrolysis temperature ( $A$ ), liquid–solid ratio ( $B$ ) and hydrolysis time ( $C$ ), were chosen in experiments according to the results of preliminary studies. The matrix of design is shown in Table 2, including the coded and actual values of these three variables [17,22].

**Table 2** Coding of experimental factors and levels

Coded value	$A/^\circ\text{C}$	$B/(\text{mL}\cdot\text{g}^{-1})$	$C/\text{min}$
1.68	30	5	10
1	50	10	30
0	70	15	50
-1	90	20	70
-1.68	100	25	90

The experimental procedures were carried out in a 250 mL spherical glass reactor equipped with a temperature control unit. Deionized water was poured into the reactor at the designated liquid–solid ratio. When the reaction temperature achieved the set values, the dross (5 g) was added to the reactor. The residue after AlN hydrolysis was removed to filter and dry at 60  $^\circ\text{C}$

for 48 h for fractal geometry analysis.

## 2.3 Analysis

The microstructure of the dross was determined using a scanning electron microscope (JSM-6360 V, Japan). The mineral phases of the dross were analyzed using an X-ray diffractometer (D/MAX 2500X, Japan) using  $\text{Cu K}\alpha$  as the radiation source at 40 mA and 200 kV. The elemental contents of the dross were examined using X-ray fluorescence (XRF-AXIOS, PANalytical, Netherlands), and the particle size distribution was measured using a laser particle analyser (OMEC LS-POP, China).

The relationship between the three independent variables and the fractal dimensions of residue from secondary aluminium dross was shown as follows:

$$Y = B_0 + \sum B_i x_i + \sum B_{ii} x_i^2 + \sum B_{ij} x_i x_j + \varepsilon \quad (3)$$

where  $Y$  is the response variable;  $B_0$  is the model constant;  $B_i$ ,  $B_{ii}$  and  $B_{ij}$  are the linear, quadratic and interactive coefficients, respectively;  $x_i$  and  $x_j$  are different independent variables ( $i \neq j$ ) and  $\varepsilon$  is error.

The optimization of multiple responses was performed using the desirability functions. Particularly, the following minimization function was used to minimize the response [19,21]:

$$d(x_i) = \begin{cases} 1, & x_i \leq L \\ (x_i - L)/(U - L), & L < x_i < U \\ U, & x_i > U \end{cases} \quad (4)$$

$$d(x_i) = \begin{cases} 1, & x_i \geq U \\ (U - x_i)/(U - L), & L < x_i < U \\ 0, & x_i \leq L \end{cases} \quad (5)$$

where  $L$  and  $U$  are the lower and upper bonds of the independent variables, respectively. The central composite design using response surface methodology was used for determining the effect of AlN hydrolysis on fractal dimensions of residue from the dross.

The fractal dimensions describe the particle size distribution:

$$S(x) = k(x/X)^{3-D} \quad (6)$$

where  $S(x)$  is the granularity of cumulative distribution function, %;  $D$  is the fractal dimension;  $k$  is the slope;  $x$  is the diameter of particle size,  $\mu\text{m}$ ; and  $X$  is the maximum value of the particle diameter,  $\mu\text{m}$ . Logarithms on both sides were determined as follows:

$$\lg S(x) = \lg k + (3-D)(\lg x - \lg X) \quad (7)$$

With the further development:

$$\lg S(x) = \lg k_1 + (3-D)\lg x \quad (8)$$

Then, the plot of  $\lg S(x)$  vs  $\lg x$  was taken, and from slope we can calculate the  $D$  value.

### 3 Results and discussion

#### 3.1 Thermodynamic calculation of AlN hydrolysis

The Gibbs free energy in a metallurgical thermodynamics process at different temperatures was calculated using the following equations [12]:

$$H_n^\ominus(T) = \Delta_f H_n^\ominus + \int_{298}^T c_p dT \quad (9)$$

$$\Delta H^\ominus = \sum v_n H_n^\ominus(T) \quad (10)$$

$$S_n^T(T) = S_{n,298}^\ominus + \int_{298}^T c_p d \ln T + \sum \frac{\Delta H_n^t}{T_n} \quad (11)$$

$$\Delta S^\ominus = \sum v_n S_n^\ominus(T) \quad (12)$$

$$\Delta G^\ominus = \Delta H^\ominus - T \Delta S^\ominus \quad (13)$$

After AlN reacted with water, the reaction was as Eq. (1).

From Table 3, the Gibbs free energy values of the reaction were  $-217.54$ ,  $-211.05$ ,  $-204.51$ ,  $-197.91$  and  $-194.59$  kJ/mol at 303, 323, 343, 363 and 373 K, respectively, after calculation, which indicated that the AlN hydrolysis reaction (1) could have occurred at standard conditions.

**Table 3** Thermodynamic parameters for AlN, H<sub>2</sub>O, Al(OH)<sub>3</sub> and NH<sub>3</sub>, respectively [12]

Substance	$c_p$	$H_{298}^\ominus /$ (kJ·mol <sup>-1</sup> )	$S_{298}^\ominus /$ (kJ·mol <sup>-1</sup> ·K <sup>-1</sup> )
AlN	$32.267 + 22.686 \times 10^{-3} T - 7.904 \times 10^5 T^{-2}$	-317.98	20.15
H <sub>2</sub> O	$29.999 + 10.711 \times 10^{-3} T + 0.335 \times 10^5 T^{-2}$	-241.81	188.72
Al(OH) <sub>3</sub>	$30.602 + 209.786 \times 10^{-3} T$	-1284.49	71.13
NH <sub>3</sub>	$25.794 + 31.623 \times 10^{-3} T + 0.351 \times 10^5 T^{-2}$	-45.94	192.67

#### 3.2 Characterizations of residue hydrolysed from secondary aluminium dross

The diffraction peak intensity of AlN in residue hydrolysed at 30 °C, with a liquid–solid ratio of 5 mL/g for 10 min was weaker than that of the original secondary aluminium dross (Fig. 2). The contents of AlN in residue were reduced while the Al(OH)<sub>3</sub> was not evident, which indicates that it may have changed into the amorphous AlOOH [11] or that its content was too small. At the same time, the peaks of MgAl<sub>2</sub>O<sub>4</sub> spinel and corundum found in the residue showed that the compounds of MgAl<sub>2</sub>O<sub>4</sub> spinel and corundum were stable.

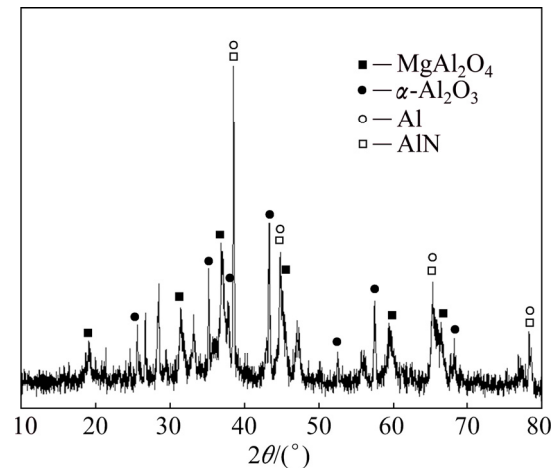
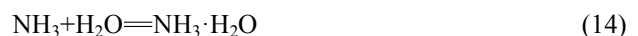


**Fig. 2** XRD pattern of dross after hydrolysis

Figure 3 shows the SEM images of the dross before and after hydrolysis. The microstructure of the dross before hydrolysis was rough, angular, irregular and porous, while it became smooth after hydrolysis once the particles of the residue reacted together. The element Al mainly covered the dross particle before hydrolysis while it existed mainly in MgAl<sub>2</sub>O<sub>4</sub> spinel and corundum after hydrolysis. The distribution of the element Al in the residue was uniform.

#### 3.3 Fractal dimension characteristics of hydrolysed dross

The hydrolysis of AlN was employed using response surface modelling, and the oval of contour plots indicated by cross-action was obvious ( $p < 0.01$ ) [23,24]. The 3D surface graphs and counter plots shown in Fig. 4 (A) display the dimensions based on the temperature and liquid–solid ratios. The fractal dimensions changed significantly due to the liquid–solid ratio of deionized water to dross. When the hydrolysis time was constant at 50 min and the hydrolysis temperature was raised from 30 to 100 °C, the fractal dimensions of residue decreased from approximately 1.7 to 1.3. According to the reaction of AlN hydrolysis from the dross, it was beneficial to form the phase of Al(OH)<sub>3</sub> with high temperature, which is helpful to maintain homogeneity in the residue. When the liquid–solid ratio of the deionized water to dross varied from 25 to 5 mL/g, the fractal dimensions of residue were also decreased from approximately 1.7 to 1.3. The fractal dimensions of the residue decreased as the liquid–solid ratio decreased [12]. The results may be attributed to Eq. (1) and following reactions:



which decrease the size and homogeneity of the residue.

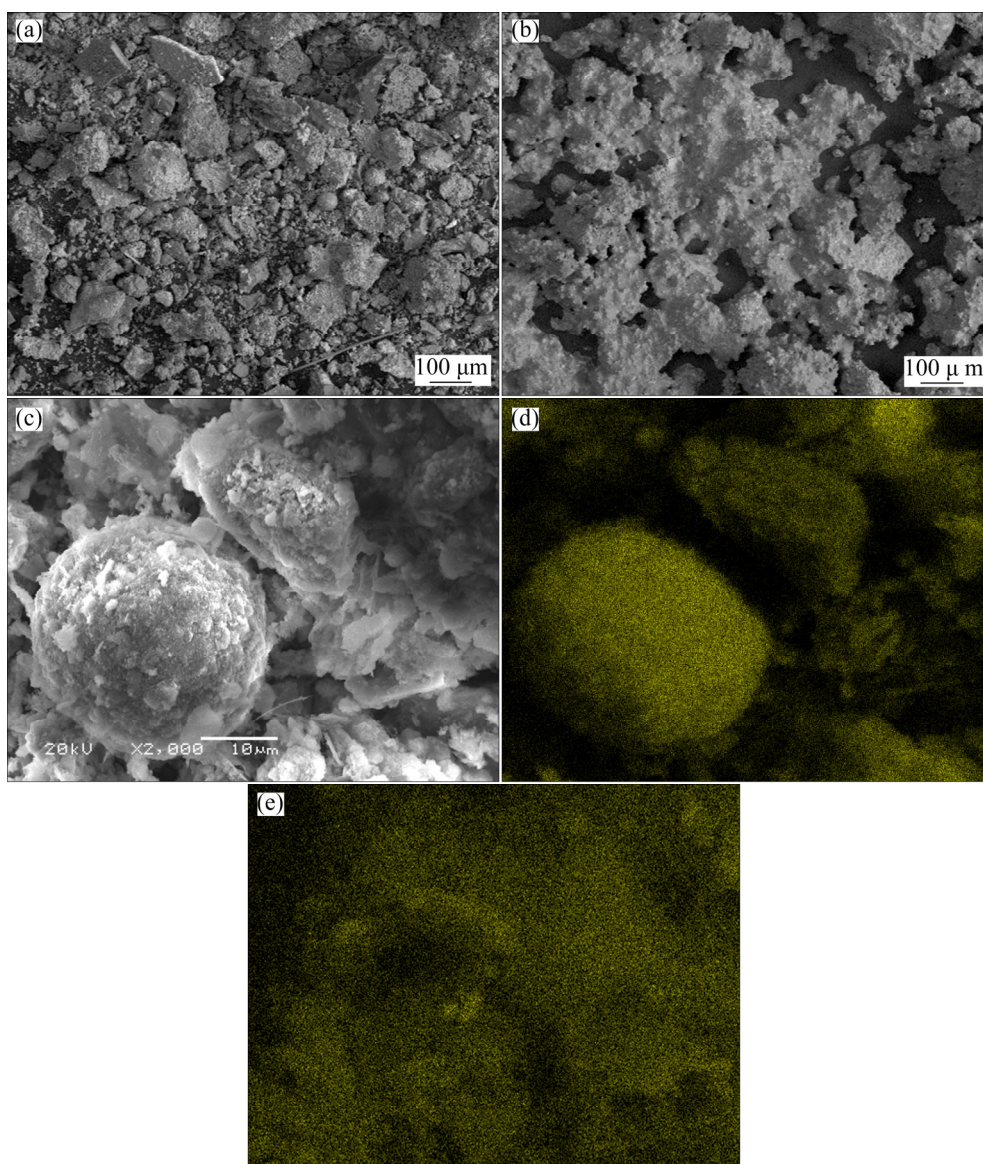


**Fig. 3** SEM images (a, b, c) and element Al mapping analysis (d, e) of dross before (a, c, d) and after (b, e) hydrolysis

The 3D surface graphs and counter plots shown in Fig. 4(b) display the fractal dimensions based on the temperature and time. The fractal dimensions of the residue changed significantly through the interaction between hydrolysis temperature and time. When the liquid–solid ratio was constant at 15 mL/g and temperature changed from 30 to 65 °C, the fractal dimensions of residue increased from approximately 1.6 to 1.7 when the hydrolysis time ranged from 10 to 50 min, and the fractal dimensions of residue increased from approximately 1.7 to 1.8 when the hydrolysis time varied from 50 to 90 min. When the temperature changed from 65 to 100 °C, however, the fractal dimensions of residue decreased from approximately 1.7 to 1.5, and the hydrolysis time shifted from 10 to 90 min. These results show that the fractal dimensions of the residue are changed slightly by hydrolysis time and that the

interaction between temperature and time is significant. Amorphous  $\text{Al}(\text{OH})_3$  was found after 192 h, while crystalline bayerite  $\text{Al}(\text{OH})_3$  was detected after 250 h [25]. Aluminium oxide or a thin hydroxide shell formed on the surface of the dross after the AlN reacted with deionized water. The shell thus acted as a hydrophobic coating and prevented further reactions between the AlN with deionized water. This shell probably acted as the surface boundary layer on the dross particle [26], causing resistance of AlN between the dross and the deionized water. At higher temperatures, the deionized water might smoothly and quickly penetrate the AlN particle [11]. The fractal dimensions of the residue decreased with prolonged time at higher temperatures. High hydrolysis temperature increased the hydrolysis rate and extended the hydrolysis time, facilitating the reactions (1), (14) and (15).

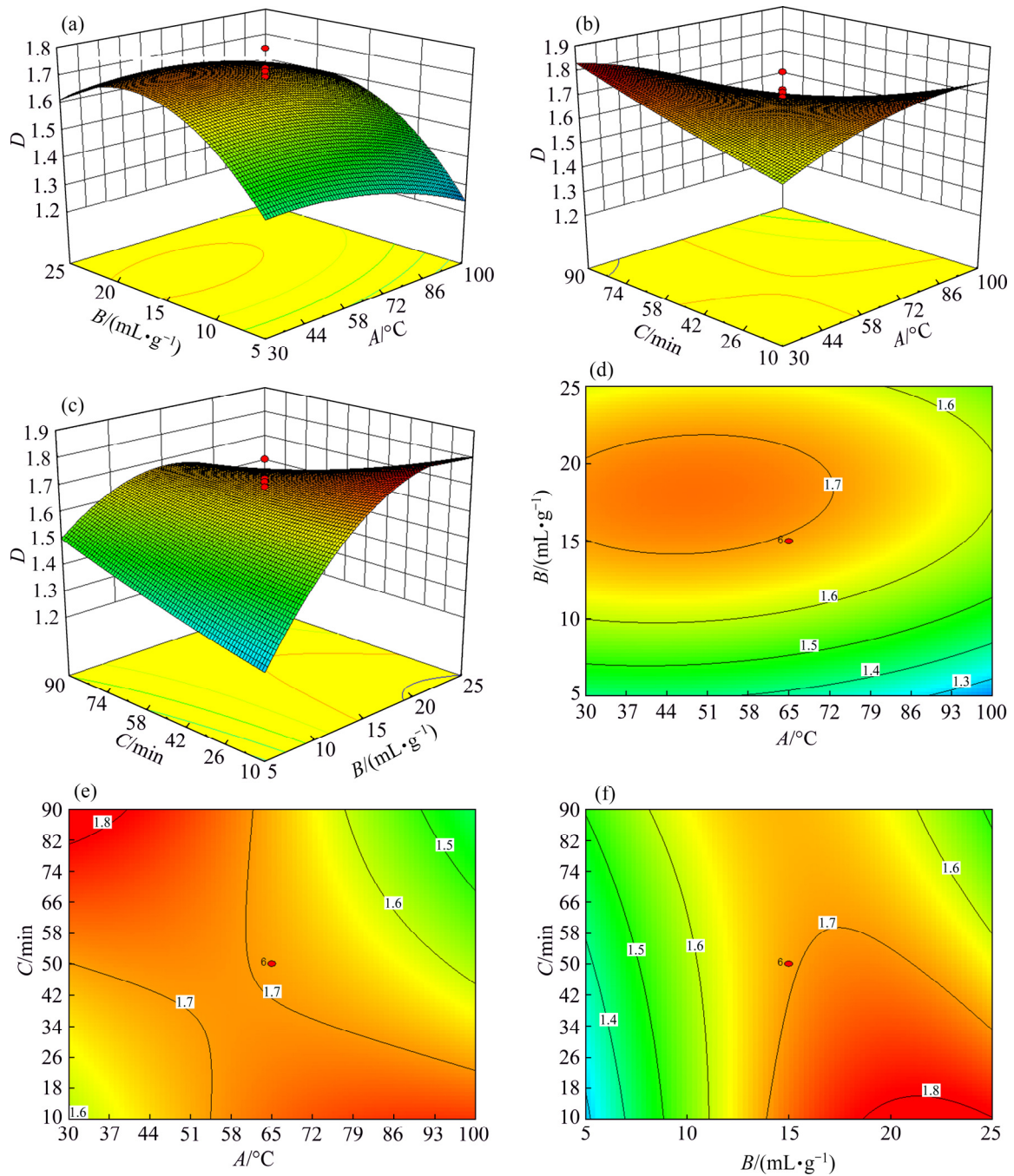


**Fig. 4** Three-dimensional response plots (a, b, c) and two-dimensional contour plots (d, e, f) for disintegration: (a, d) Temperature and liquid–solid ratio at hydrolysis time of 50 min; (b, e) Temperature and hydrolysis time at liquid–solid ratio of 15 mL/g; (c, f) Liquid–solid ratio and hydrolysis time at temperature of 65  $^{\circ}\text{C}$

Similarly, the 3D surface graphs and counter plots shown in Fig. 4(c) display the dimensions based on the liquid–solid ratios and time. When the hydrolysis temperature was constant at 65  $^{\circ}\text{C}$ , when the hydrolysis time changed from 10 to 50 min, the fractal dimensions of residue increased from approximately 1.3 to 1.6 and the liquid–solid ratio varied from 5 to 15 mL/g, and when the fractal dimensions of residue increased from approximately 1.7 to 1.8 the liquid–solid ratio varied

from 15 to 25 mL/g. When the hydrolysis time changed from 50 to 90 min, the fractal dimensions of residue increased from approximately 1.3 to 1.6 and the liquid–solid ratio varied from 5 to 15 mL/g, and when the fractal dimensions of residue decreased from approximately 1.7 to 1.6, the liquid–solid ratio shifted from 15 to 25 mL/g. These results show that the fractal dimensions of the residue significantly changed due to the liquid–solid ratio of deionized water to the dross and

the interaction between liquid–solid ratio and time.

From Table 4, the actual fractal dimensions of residue changed from 1.16 to 1.80. The fractal dimensions of residue were significantly affected by the liquid–solid ratio of deionized water to dross ( $p<0.05$ ), the interaction between hydrolysis temperature and hydrolysis time ( $p<0.01$ ) and the interaction between liquid–solid ratio and hydrolysis time ( $p<0.01$ ), respectively. These results show that the fractal dimensions of residue from secondary aluminium dross can be optimized using the AlN hydrolysis of the dross.

The relationship between the independent variables and the fractal dimensions was expressed by the following quadratic regression equation:

$$D=0.52+8.47\times 10^{-3}A+0.08B+0.01C+6.07\times 10^{-5}AB-1.04\times 10^{-4}AC-3.34\times 10^{-4}BC-4.54\times 10^{-5}A^2-1.89\times 10^{-3}B^2+7.39\times 10^{-6}C^2 \quad (R^2=0.90) \quad (16)$$

The actual data were carefully fitted agreeing with

**Table 4** Results analysis based on orthogonal rotational experiments

Experimental No.	A/ °C	B/ (mL·g <sup>-1</sup> )	C/ min	Actual D	Calculated D
1	65	15	50	1.61	1.64
2	65	15	50	1.72	1.64
3	100	25	90	1.30	1.16
4	65	15	50	1.73	1.64
5	6.14	15	50	1.50	1.59
6	100	5	10	1.29	1.28
7	65	15	50	1.63	1.64
8	30	5	10	1.16	1.15
9	100	25	10	1.79	1.80
10	30	25	10	1.75	1.58
11	65	15	50	1.80	1.64
12	65	15	117.27	1.62	1.61
13	65	31.82	50	1.30	1.29
14	30	25	90	1.67	1.53
15	100	5	90	1.16	1.17
16	65	15	50	1.70	1.64
17	30	5	90	1.79	1.62
18	123.86	15	50	1.51	1.38

Source	Means square	F value	Prob>F
A–A	0.05	4.09	0.0777
B–B	0.13	10.99	0.0106*
C–C	$5.39\times 10^{-3}$	0.44	0.5264
AB	$3.83\times 10^{-3}$	0.31	0.5917
AC	0.17	13.93	0.0058**
BC	0.15	11.87	0.0088**

Note: \*:  $p<0.05$ ; \*\*:  $p<0.01$

the calculated values, which included the relative error of the average value for the fractal dimensions of only 4.56%, and the fractal dimensions of residue were predicted according to the quadratic regression equation. Using Matlab optimization toolbox, the minimum fractal dimension of residue was 1.15 at 30 °C with the liquid–solid ratio of 5 mL/g for 10 min and the maximum fractal dimension of residue was 1.82 at 96 °C with the liquid–solid ratio of 22 mL/g for 10 min.

In conclusion, the response surface methodology was developed to investigate the effects of AlN hydrolysis on the fractal dimensions of the residue from secondary aluminium dross. The liquid–solid ratio was the main effect on the fractal dimensions of residue. The interaction between hydrolysis temperature and hydrolysis time and the interaction between liquid–solid ratio and the hydrolysis time should be considered. The homogenization of the residue promotes the reutilization of the dross and may enhance the properties of the sinters. The smaller the particle size is, the possibly higher the surface area and disordered structure are [8,9], which all contribute to a reduced sintering temperature and a higher chemical reactivity in follow-up processing.

## 4 Conclusions

1) The actual fractal dimensions of residue changed from 1.16 to 1.80 after AlN hydrolysis from secondary aluminium dross. The fractal dimensions were affected by the liquid–solid ratio ( $p<0.05$ ), the interaction between hydrolysis temperature and hydrolysis time and the interaction between liquid–solid ratio and hydrolysis time ( $p<0.01$ ).

2) The relationship between the independent variables of the AlN hydrolysis from secondary aluminium dross and the fractal dimensions was expressed using the quadratic regression equation. The fractal dimensions of residue were optimized using response surface methodology to confirm the conditions of AlN hydrolysis from secondary aluminium dross.

## References

- [1] MURAYAMA N, MAEKAWA I, USHIRO H, MIYOSHI T, SHIBATA J, VALIX M. Synthesis of various layered double hydroxides using aluminum dross generated in aluminum recycling process [J]. International Journal of Mineral Processing, 2012, 110–111(18): 46–52.
- [2] LÓPEZ-DELGADO A, TAYIBI H, PÉREZ C, ALGUACIL F J, LÓPEZ F A. A hazardous waste from secondary aluminium metallurgy as a new raw material for calcium aluminate glasses [J]. Journal of Hazardous Materials, 2009, 165(1–3): 180–186.
- [3] SHINZATO M C, HYPOLITO R. Solid waste from aluminum recycling process: Characterization and reuse of its economically valuable constituents [J]. Waste Management, 2005, 25(1): 37–46.
- [4] TSAKIRIDIS P E. Aluminium salt slag characterization and utilization—A review [J]. Journal of Hazardous Materials, 2012,

- 217–218(6): 1–10.
- [5] TSAKIRIDIS P E, OUSTADAKIS P, AGATZINI-LEONARDOU S. Aluminium recovery during black dross hydrothermal treatment [J]. Journal of Environmental Chemical Engineering, 2013, 1(1–2): 23–32.
- [6] CALDER G V, STARK T D. Aluminum reactions and problems in municipal solid waste landfills [J]. Practice Periodical of Hazardous, Toxic, and Radioactive Waste Management, 2010, 14(4): 258–265.
- [7] XIAO Yan-ping, REUTER M A, BOIN U. Aluminium recycling and environmental issues of salt slag treatment [J]. Journal of Environmental Science and Health, Part A, 2005, 40(10): 1861–1875.
- [8] DAVID E, KOPAC J. Hydrolysis of aluminum dross material to achieve zero hazardous waste [J]. Journal of Hazardous Materials, 2012, 209–210(4): 501–509.
- [9] DASH B, DAS B R, TRIPATHY B C, BHATTACHARYA I N, DAS S C. Acid dissolution of alumina from waste aluminium dross [J]. Hydrometallurgy, 2008, 92(1–2): 48–53.
- [10] LI Peng, GUO Min, ZHANG Mei, TENG Li-dong, SEETHARAMAN S. Leaching process investigation of secondary aluminum dross: The effect of CO<sub>2</sub> on leaching process of salt cake from aluminum remelting process [J]. Metallurgical and Materials Transactions B, 2012, 43(5): 1220–1221.
- [11] FUKUMOTO S, HOOKABE T, TSUBAKINO H. Hydrolysis behavior of aluminum nitride in various solutions [J]. Journal of Materials Science, 2000, 35(11): 2743–2748.
- [12] JIANG Lan, QIU Ming-fang, DING You-dong, SU Nan, YAO Quan. Hydrolysis behavior of AlN in aluminum dross [J]. The Chinese Journal of Nonferrous Metals, 2012, 22(12): 3555–3557. (in Chinese)
- [13] NAN Jun, HE Wei-peng, ZHANG Zhi-jun, LI Gui-bai. Fractal characteristics of particle size distribution in dynamic flocculation process [J]. Wuhan University Journal of Natural Sciences, 2009, 14(6): 511–517.
- [14] ZHOU Zi-long, DU Xue-ming, WANG Shan-yong, CAI Xin, CHEN Zhao. Cement grout transport within sand with fractal characteristics considering filtration [J]. European Journal of Environmental and Civil Engineering, 2017, 21: 1–23.
- [15] ZHOU Zi-long, DU Xue-ming, CHEN Zhao, ZHAO Yun-long. Grouting diffusion of chemical fluid flow in soil with fractal characteristics [J]. Journal of Central South University, 2017, 24(5): 1190–1196.
- [16] CAO Jing-ya, WU Qian-hong, LI Huan, OUYANG Cheng-xin, KONG Hua, XI Xiao-shuang. Metallogenic mechanism of Pingguo bauxite deposit, western Guangxi, China: Constraints from REE geochemistry and multi-fractal characteristics of major elements in bauxite ore [J]. Journal of Central South University, 2017, 24(7): 1627–1636.
- [17] XU Chao, WANG Jing-jing, YANG Ti-long, CHEN Xia, LIU Xun-yue, DING Xing-cheng. Adsorption of uranium by amidoximated chitosan-grafted polyacrylonitrile, using response surface methodology [J]. Carbohydrate Polymers, 2015, 121: 79–85.
- [18] AZIZI D, SHAFAEI S Z, NOAPARAST M, ABDOLLAHI H. Modeling and optimization of low-grade Mn bearing ore leaching using response surface methodology and central composite rotatable design [J]. Transactions of Nonferrous Metals Society of China, 2012, 22(9): 2295–2305.
- [19] LI Zhi-qiang, LI Jing, ZHANG Li-bo, PENG Jin-hui, WANG Shi-xing, MA Ai-yuan, WANG Bao-bao. Response surface optimization of process parameters for removal of F and Cl from zinc oxide fume by microwave roasting [J]. Transactions of Nonferrous Metals Society of China, 2015, 25(3): 973–980.
- [20] YANG Ke-di, YE Xian-jia, SU Jing, SU Hai-feng, LONG Yun-fei, LV Xiao-yan, WEN Yan-xuan. Response surface optimization of process parameters for reduction roasting of low-grade pyrolusite by bagasse [J]. Transactions of Nonferrous Metals Society of China, 2013, 23(2): 548–555.
- [21] LI Ying-wei, PENG Jin-hui, LIANG Gui-an, LI Wei, ZHANG Shi-min. Optimization of processing parameters for microwave drying of selenium-rich slag using incremental improved back-propagation neural network and response surface methodology [J]. Journal of Central South University of Technology, 2011, 18(5): 1441–1442.
- [22] FAN Tao, HU Jian-guo, FU Li-dan, ZHANG Li-jin. Optimization of enzymolysis-ultrasonic assisted extraction of polysaccharides from *Momordica charabtia* L. by response surface methodology [J]. Carbohydrate Polymers, 2015, 115: 701–706.
- [23] YANG Ke-di, TAN Fang-xiang, WANG Fan, LONG Yun-fei, WEN Yan-xuan. Response surface optimization for process parameters of LiFePO<sub>4</sub>/C preparation by carbothermal reduction technology [J]. Chinese Journal of Chemical Engineering, 2012, 20(4): 793–802.
- [24] DEROSI A, SEVERINI C, MASTRO A D, PILLI T D. Study and optimization of osmotic dehydration of cherry tomatoes in complex solution by response surface methodology and desirability approach [J]. LWT-Food Science and Technology, 2015, 60(2): 641–648.
- [25] ZHANG Yong-heng, BINNER J. Hydrolysis process of a surface treated aluminum nitride powder-a FTIR study [J]. Journal of Materials Science Letters, 2002, 21(10): 803–805.
- [26] CHANDLER H D. Activation entropy and anomalous temperature dependence of viscosity in aqueous suspensions of Fe<sub>2</sub>O<sub>3</sub> [J]. Powder Technology, 2017, 305: 572–577.

## 响应曲面法研究二次铝灰中 AlN 水解对水解后残渣分形维数的影响

张勇, 郭朝晖, 韩自玉, 肖细元

中南大学 冶金与环境学院, 长沙 410083

**摘要:** 利用响应曲面方法研究二次铝灰中 AlN 水解条件对水解后残渣分形维数的影响。研究表明, AlN 水解显著影响水解后残渣分形维数。在 303~373 K 温度下, AlN 水解标准状态下可自发进行, 水解液固比显著影响水解后残渣分形维数( $p < 0.05$ ), 残渣维数实际变化范围为 1.16~1.80, 与计算值吻合度较高。此外, 水解温度与水解时间之间交互作用, 液固比与水解时间之间交互作用影响水解后残渣分形维数( $p < 0.01$ )。当二次铝灰中 AlN 水解优化条件为水解温度 30 °C、水解液固比 5 mL/g 和水解时间 10 min 时, 残渣最小分形维数达到 1.15。为提高二次铝灰综合利用, 响应曲面法可以优化 AlN 水解条件以获得较小分形维数的残渣。

**关键词:** 二次铝灰; AlN 水解; 分形维数; 优化; 响应曲面

(Edited by Xiang-qun LI)